Applied Mathematical Modelling 40 (2016) 5497–5509

Contents lists available at ScienceDirect

Applied Mathematical Modelling

journal homepage: www.elsevier.com/locate/apm

A new analytical solution for agglomerate growth undergoing Brownian coagulation

Mingzhou Yu[a,b,*], Yueyan Liu[a], Guodong Jin[b], Hanhui Jin[c,**]

[a] China Jiliang University, Hangzhou 310028, China
[b] The State Key Laboratory of Nonlinear Mechanics, Chinese Academy of Sciences, Beijing 100090, China
[c] Institute of Fluid Engineering, Zhejiang University, Hangzhou 310017, China

ARTICLE INFO

Article history:
Received 27 April 2015
Revised 17 December 2015
Accepted 8 January 2016
Available online 18 January 2016

Keywords:
Agglomerate
Population balance equation
Analytical solution
Brownian coagulation
Continuum-slip regime

ABSTRACT

We proposed a new analytical solution for a population balance equation for fractal-like agglomerates. The new analytical solution applies to agglomerates with any mass fractal dimensions. Two well-known numerical methods, including the Taylor-series expansion method of moments and the quadrature method of moments, were selected as references. The reliability of the analytical solution with three mass fractal dimensions of 1.0, 2.0, and 3.0 in the continuum-slip regime was verified. The accuracy of the new analytical solution is affected by both the Knudsen number and the mass fractal dimension. The new analytical solution can be further improved in accuracy by introducing a correction factor to the originally derived mathematical formula. The new analytical solution was finally confirmed to possess potential for replacing the numerical solution in the continuum-slip regime.

1. Introduction

Aerosols are unstable in particle process engineering and the environment because of Brownian coagulation, which causes the particle size distribution to always vary with time [1]. This process can be characterized mathematically by solving the the population balance equation (PBE) [2,3]. The PBE was proposed by Smoluchowski and later developed by Müller in its integral-differential form [4,5]. However, the PBE associated with a particle-size-dependent coagulation kernel cannot be precisely solved. Various methods for solving the PBE have been proposed in the last century, including the method of moments [6–11], sectional method [12–15], and Monte Carlo method [16–19], with almost all methods belonging to the numerical solution. For the numerical solution, time-consuming iterative algorithms, such as the 4th-order Runge–Kutta method, must be performed. Although there are also some analytical solutions [20–22], the scope of their application is usually limited because of their inability to resolve time-dependent dynamical process or because of a prior assumption about size distribution. For fractal-like agglomerates, the analytical solution for the PBE is more difficult to achieve because of an additional variable(i.e., the mass fractal dimension) [2].

* Corresponding author at: Zhejiang University, Hangzhou, China (HH); China Jiliang University, Hangzhou, China (MZ), Tel: +8613758136221.
** Corresponding author.
E-mail addresses: yumz@ieecas.cn (M. Yu), enejhh@zju.edu.cn (H. Jin).

http://dx.doi.org/10.1016/j.apm.2016.01.009
S0307-904X(16)00013-5/

Nomenclature

A	constant (=1.591)
r	particle radius, m
N	particle number concentration density, m^{-3}
B_2	collision coefficient for the continuum-slip regime
C	Cunningham correction factor
k_b	Boltzmann constant, J K
Kn	particle Knudsen number
m_k	kth moment of particle size distribution
g	$=m_0m_2/m_1^2$
M_k	Dimensionless kth moment of size distribution
t	time, s
T	temperature, K
U	the point of Taylor-series expansion (m_1/m_0)
v	particle volume, m^3
v_g	geometric mean particle volume, m^3
N	initial total particle number concentration, m^{-3}
f	$1/D_f$
D_f	mass fractal dimension
Greek letters	
ν	kinematic viscosity, $m^2\ s^{-1}$
B	particle collision kernel
M	gas viscosity, $kg\ m^{-1}\ s^{-1}$
λ	mean free path of the gas, m
σ_g	geometric mean deviation of size distribution
τ	dimensionless coagulation time, tN_0B_2

Because of the relative simplicity of implementation and the low computational cost, the method of moments has been extensively used to resolve aerosol dynamical processes [23]. In the application of this method, the fractal moment variables inevitably appear in the conversion from the PBE to the ordinary differential equations (ODEs) for kth moments, the closure of which can be achieved using five techniques [23](i.e., pre-defined size distributed method [9,24], Gaussian quadrature method (QMOM) [8,10], pth-order polynomical method [25], interpolative method [7], and Taylor-series expansion method (TEMOM) [11,26]). To the best of our knowledge, the TEMOM has the simplest structure for governing equations among all the methods of moments. Compared with the QMOM and its variants, such as the direct QMOM, the TEMOM has an advantage in analytically expressing the time evolution of kth moments as polynomials composed of integer moments. Thus, the ODEs of the TEMOM are more easily solved analytically compared with their counterparts, especially for fractal-like agglomerates involving a very complex coagulation kernel.

Since being proposed in 2008 [11], the TEMOM has displayed potential to become a vital method in solving the PBE because it makes no assumptions for size distribution and generates very low computational costs. Two key physical quantities characterizing an aerosol property (the geometric standard deviation [GSD] of number distribution and geometric mean volume) [27] can be easily reconstructed using this method. In fact, the TEMOM, QMOM, and log-normal method of moments (log MM) [9] have been verified to yield nearly the same results for both quantities as well as for the first three moments [28]. Along with a mathematical analysis of the ODEs of the TEMOM, the governing equations for kth moments can be further simplified through introducing a novel variable $g(m_0m_2/{m_1}^2$, where m_0, m_1, and m_2 are the first three moments, respectively). It was recently verified that if g is treated as a constant, then the ODEs of the TEMOM can be analytically resolved by executing a separate variable method (SPV) in both the continuum regime and free molecular regime [31]. Primarily because of the novel property of g, it only varies within a very small range, as illustrated in Fig. 1. This is consistent with the self-preserving size distribution theory first devised by Friedlander [22]. However, the feasibility of treating g as a constant in the derivation for fractal-like agglomerates in the continuum-slip regime has never been verified.

Therefore, the aim of this study was to verify the feasibility of an analytical solution for solving the PBE for fractal-like agglomerates in the continuum-slip regime. Here, fractal-like agglomerates represent particles composed of numerous smaller primary particles, the morphology of which can be characterized using fractal theory. Because the TEMOM and QMOM for numerically solving ODEs have been verified as reliable solutions [6–11], they were used here as references. Three key physical quantities, namely the total particle number concentration, GSD of the number distribution, and geometric volume concentration, were chosen for investigation. The structure of this paper is as follows. In Section 2, the mathematical equations are briefly discussed, and in Section 3, the specific calculation parameters are given. The results and discussion are presented in Section 4. Conclusions are given in Section 5.

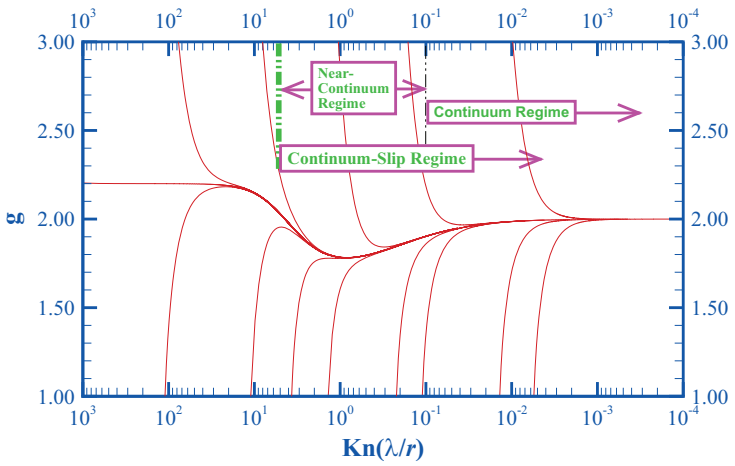

Fig. 1. Variance of g with different initial values by solving the PBE undergoing Brownian coagulation. Kn is the Knudsen number, $Kn = \lambda/r$, where λ is mean free path of air molecular and r is the radius of an aerosol particle.

2. Mathematical model

The PBE was first proposed by Smoluchowski and then developed by Müller into its integral-differential form [4,5],

$$\frac{\partial n(v,t)}{\partial t} = \frac{1}{2}\int_0^v \beta\left(v-v',v'\right)n\left(v-v',t\right)n\left(v',t\right)dv' - n(v,t)\int_0^\infty \beta\left(v,v'\right)n\left(v',t\right)dv', \tag{1}$$

where $n(v, t)dv$ is the particle number whose volume is between v and $v + dv$ at time t, and $\beta(v, v')$ is the collision kernel for two particles of volumes v and v'. In the continuum-slip regime, the form of the collision kernel for fractal agglomerates is as follows [26]:

$$\beta\left(v,v'\right) = B_2\left\{\left(\frac{1}{v^f}+\frac{1}{v'^f}\right)\left(v^f+v'^f\right) + \emptyset v_{p0}{}^{f-\frac{1}{3}}\left(\frac{1}{v^{2f}}+\frac{1}{v'^{2f}}\right)\left(v^f+v'^f\right)\right\}, \tag{2}$$

where v_c is the collision volume of agglomerates with $v_c = v_{p0}{}^{1-3/D_f} v^{3/D_f}$, $\emptyset = \lambda A/(3/4\pi)^{1/3}$, $A = 1.591$, $f = 1/D_f$, and v is the real volume of the agglomerate. Here, v_{p0} is the volume of primary particles whose diameter is specified to be 1 nm in this work, and and D_f is the fractal dimension, whose value is theoretically between 1 and 3. $B_2 = 2k_BT/3\mu$, where k_B is the Boltzmann constant, T denotes the air temperature, and μ denotes the gas viscosity. As Eq. (2) is introduced into Eq. (1), and the method of moments is applied,

$$\frac{\partial m_k}{\partial t} = \frac{1}{2}\int_0^\infty\int_0^\infty [(v+v')^k - v^k - v'^k]\beta(v,v')n(v,t)n(v',t)dvdv' \ (k = 0,1,2,\ldots), \tag{3}$$

where the moment,m_k, is defined by,

$$m_k = \int_0^\infty v^k n(v)dv. \tag{4}$$

To obtain the closure of Eq. (3), we must introduce the closure model for kth moments [11],

$$m_k = u_0{}^{k-2}\left(\frac{k^2-k}{2}\right)m_2 + u_0{}^{k-1}\left(-k^2+2k\right)m_1 + u_0{}^k\left(\frac{k^2-3k}{2}\right)m_0 \tag{5}$$

Here, the Taylor-series expansion point, u, is calculated as averaged volume, $u = m_1/m_0$. Although the geometric mean volume, $({m_1}^2/({m_0}^{3/2}{m_1}^{1/2})$, seems more reasonable than the averaged volume, it cannot reach the expected level in the TEMOM. The theoretical analysis of selecting these two volumes as Taylor-series expansion points has been conducted in [29] and [30], in which the averaged volume has been verified as a more precise measure. Although the highest order of moments in Eq. (5) is two, it was verified to reliably approximate moments with orders up to $2+f$, which is the highest order that appears in the investigated model in this work [26].Applying Eq. (2) to Eq. (3) and further approximating fractal

moments by using Eq. (5), we obtain,

$$\begin{cases} \dfrac{dm_0}{dt} = B_2 \left\{ \begin{array}{l} \left(\dfrac{-f^4+f^2}{4}g^2 + \dfrac{f^4-3f^2}{2}g + \dfrac{-f^4+5f^2-8}{4} \right) m_0^2 + \phi \nu_{p0}^{f-1/3} \left(\dfrac{g m_1}{m_2} \right)^f \\ \left[\left(-f^4 + \dfrac{1}{2}f^3 + \dfrac{1}{2}f^2 \right) g^2 + \left(2f^4 - f^3 - 4f^2 - f \right) g + \left(-f^4 + \dfrac{1}{2}f^3 + \dfrac{7}{2}f^2 + f - 2 \right) \right] m_0^2 \end{array} \right\} \\ \dfrac{dm_1}{dt} = 0 \\ \dfrac{dm_2}{dt} = B_2 \left\{ \begin{array}{l} \left(\dfrac{f^4-f^2}{2}g^2 + \left(-f^4+3f^2 \right) g + \dfrac{f^4-5f^2+8}{2} \right) m_1^2 + \phi \nu_{p0}^{f-1/3} \left(\dfrac{g m_1}{m_2} \right)^f \\ \left[\left(2f^4 + f^3 - f^2 \right) g^2 + \left(-4f^4 - 2f^3 + 8f^2 - 2f \right) g + \left(2f^4 + f^3 - 7f^2 + 2f + 4 \right) \right] m_1^2 \end{array} \right\} \end{cases}, \tag{6}$$

where $g = m_0 m_2 / {m_1}^2$. Our previous works provide instructions on how to use Taylor-series methods of moments to obtain closure of moment equations [11,26]. When applying a dimensionless solution with $m_k = M_k m_{k0}$ and $m_{k0} = N {v_{g0}}^k$ to Eq. (6), the dimensionless ODEs for moments are expressed as follows:

$$\begin{cases} \dfrac{dM_0}{d\tau} = \left\{ \begin{array}{l} \left(\dfrac{-f^4+f^2}{4}g^2 + \dfrac{f^4-3f^2}{2}g + \dfrac{-f^4+5f^2-8}{4} \right) {M_0}^2 + \phi \nu_{p0}^{f-1/3} (v_{g0})^{-f} \left(\dfrac{1}{M_1} \right)^f \\ \left[\left(-f^4 + \dfrac{1}{2}f^3 + \dfrac{1}{2}f^2 \right) g^2 + \left(2f^4 - f^3 - 4f^2 - f \right) g + \left(-f^4 + \dfrac{1}{2}f^3 + \dfrac{7}{2}f^2 + f - 2 \right) \right] {M_0}^{2-f} \end{array} \right\} \\ \dfrac{dM_1}{d\tau} = 0 \\ \dfrac{dM_2}{d\tau} = \left\{ \begin{array}{l} \left(\dfrac{f^4-f^2}{2}g^2 + (-f^4+3f^2) g + \dfrac{f^4-5f^2+8}{2} \right) {M_1}^2 + \phi \nu_{p0}^{f-1/3} (v_{g0})^{-f} g^f {M_1}^{2+f} \\ \left[\left(2f^4 + f^3 - f^2 \right) g^2 + \left(-4f^4 - 2f^3 + 8f^2 - 2f \right) g + \left(2f^4 + f^3 - 7f^2 + 2f + 4 \right) \right] {M_2}^{-f} \end{array} \right\} \end{cases}, \tag{7}$$

where $\tau = NB_2 t$. Here, we used the same method as in [26] to replace v_{g0} with v_{p0}, then,

$$\begin{cases} \dfrac{dM_0}{d\tau} = \left\{ \begin{array}{l} \left(\dfrac{-f^4+f^2}{4}g^2 + \dfrac{f^4-3f^2}{2}g + \dfrac{-f^4+5f^2-8}{4} \right) {M_0}^2 + AKn_0 \left(\dfrac{1}{M_1} \right)^f \\ \left[\left(-f^4 + \dfrac{1}{2}f^3 + \dfrac{1}{2}f^2 \right) g^2 + \left(2f^4 - f^3 - 4f^2 - f \right) g + \left(-f^4 + \dfrac{1}{2}f^3 + \dfrac{7}{2}f^2 + f - 2 \right) \right] {M_0}^{2+f} \end{array} \right\} \\ \dfrac{dM_1}{d\tau} = 0 \\ \dfrac{dM_2}{d\tau} = \left\{ \begin{array}{l} \left(\dfrac{f^4-f^2}{2}g^2 + (-f^4+3f^2) g + \dfrac{f^4-5f^2+8}{2} \right) {M_1}^2 + AKn_0 g^f {M_1}^{2+f} \\ \left[\left(2f^4 + f^3 - f^2 \right) g^2 + \left(-4f^4 - 2f^3 + 8f^2 - 2f \right) g + \left(2f^4 + f^3 - 7f^2 + 2f + 4 \right) \right] {M_2}^{-f} \end{array} \right\} \end{cases}, \tag{8}$$

where Kn_0 is the Knudsen number for agglomerates at an initial time. Eq. (8) is further simplified as follows:

$$\begin{cases} \dfrac{dM_0}{d\tau} = a_c {M_0}^2 + a_{cm} {M_0}^{2+f} \\ \dfrac{dM_1}{d\tau} = 0 \\ \dfrac{dM_2}{d\tau} = b_c + b_{cm} {M_2}^{-f} \end{cases}, \tag{9}$$

where

$$a_c = \left(\frac{-f^4+f^2}{4}g^2 + \frac{f^4-3f^2}{2}g + \frac{-f^4+5f^2-8}{4} \right)$$

$$a_{cm} = AKn_0 \left(\frac{1}{M_1(\tau)} \right)^f \left[\left(-f^4 + \frac{1}{2}f^3 + \frac{1}{2}f^2 \right) g^2 + \left(2f^4 - f^3 - 4f^2 - f \right) g + \left(-f^4 + \frac{1}{2}f^3 + \frac{7}{2}f^2 + f - 2 \right) \right]$$

$$b_c = \left(\frac{f^4-f^2}{2}g^2 + \left(-f^4+3f^2 \right) g + \frac{f^4-5f^2+8}{2} \right) M_1(\tau)^2$$

$$b_{cm} = AKn_0 g^f {M_1}^{2+f} \left[\left(2f^4 + f^3 - f^2 \right) g^2 + \left(-4f^4 - 2f^3 + 8f^2 - 2f \right) g + \left(2f^4 + f^3 - 7f^2 + 2f + 4 \right) \right].$$

In the evolution of an aerosol dominated by Brownian coagulation, it is feasible to assume g as a constant [31]. Under these conditions, coefficients a_c, a_{cm}, b_c, and b_{cm} are constants, and the analytical solution of Eq. (9) might be obtained:

$$\begin{cases} \int_{M_{00}}^{M_0} \dfrac{a_{cm}M_0}{a_c{M_0}^2 + a_{cm}{M_0}^{2+f}} = \int_0^{\tau} d\tau \\ M_1 = M_{10} \\ \int_{M_{20}}^{M_2} \dfrac{b_{cm}M_2}{b_c + b_{cm}{M_2}^{-f}} = \int_0^{\tau} d\tau \end{cases}, \tag{10}$$

where M_{00}, M_{10}, and M_{20} are the first three moments at an initial time. Obviously, assuming a constant g, Eq. (9) can be solved analytically and conveniently. Notably, however, g actually varies during evolution in the present model, which is discussed in Section 4.1. Therefore, the analytical solutions of the equations for M_0 and M_2 should be joined and cannot be achieved separately.

Notably, the mass fractal dimension f is a value from 1/3 to 1 [2]. Once f is specified, the analytical solution for Eq. (9) can be easily obtained. For example, we can produce the following expressions if $f = 1$,

$$\begin{cases} \tau(M_0) = \mathbb{R}(\tau) - \mathbb{R}(0) \\ \tau(M_2) = \mathbb{Z}(\tau) - \mathbb{Z}(0) \end{cases}, \tag{11}$$

with $\mathbb{R}(\tau)$ and $\mathbb{Z}(\tau)$

$$\mathbb{R}(\tau) = \frac{\ln\{(a_{cm}M_0 + a_c)/M_0\}a_{cm}}{{a_c}^2} - \frac{1}{a_cM_0},$$

and

$$\mathbb{Z}(\tau) = \frac{M_2}{b_c} - \frac{d\ln(b_cM_2 + b_{cm})}{{b_c}^2}.$$

In Eq. (11), M_0, M_1, M_2, a_c, a_{cm}, b_c, and b_{cm} are all functions of time, and τ. $\mathbb{R}(0)$ and $\mathbb{Z}(0)$ are variables at the initial condition. Similarly, if $f = 1/2$, then,

$$\mathbb{R}(\tau) = \frac{\ln\left\{\dfrac{\left(a_{cm}\sqrt{M_0} - a_c\right)M_0}{\left(a_{cm}\sqrt{M_0} + a_c\right)\left({a_{cm}}^2M_0 - {a_c}^2\right)}\right\}b^2}{{a_c}^3} + \frac{2a_{cm}}{{a_c}^2\sqrt{M_0}} - \frac{1}{a_cM_0},$$

and

$$\mathbb{Z}(\tau) = \frac{M_2}{b_c} - \frac{2\sqrt{M_2}b_{cm}}{{b_c}^2} + \frac{2d^2\ln\left(b_c\sqrt{M_2} + b_{cm}\right)}{{b_c}^3}.$$

The aforementioned derivation is straightforward and does not require any assumption about the particle size distribution, distinguishing it from the existing analytical model [34–36]. In this paper, only $f = 1$, 1/2, and 1/3 are selected as examples to verify the proposed model. These three f correspond to three types of agglomerate morphology.

3. Computations

The 4th-order Runge–Kutta method with a fixed time step of 0.0010 is used to numerically solve the TEMOM and QMOM ODEs. For all numerical and analytical solutions, the total time is up to 100. In all simulations, the temperature andpressure of the surrounding air are assumed to be 300 K and 1.0130×10^5 Pa, respectively, such that the viscosity and mean free path of the gas molecules are 1.8508×10^{-5} Pa s and 68.4133 nm, respectively. The particle density is 1000 kg/m^3. The relative error for any variable is calculated as follows [11]:

$$RE\% = \frac{\phi - \phi_{NM}}{\phi_{NM}} \times 100\%, \tag{12}$$

where ϕ is the arbitrary analytical variable and ϕ_{NM} is the referenced numerical variable. In the calculation, we assume that aerosols follow log-normal size distributions, and therefore, all initial dimensionless moments are expressed as follows:

$$\begin{cases} M_{00} = 1 \\ M_{10} = \chi \\ M_{20} = \chi^4 \end{cases}, \tag{13}$$

where $\chi = e^{{w_g}^2/2}$, $w_g = 3\ln\sigma_{g0}$, and σ_{g0} is the initial GSD of the aerosol size distribution [32]. Notably, the present model can be applied to other initial size distributions.

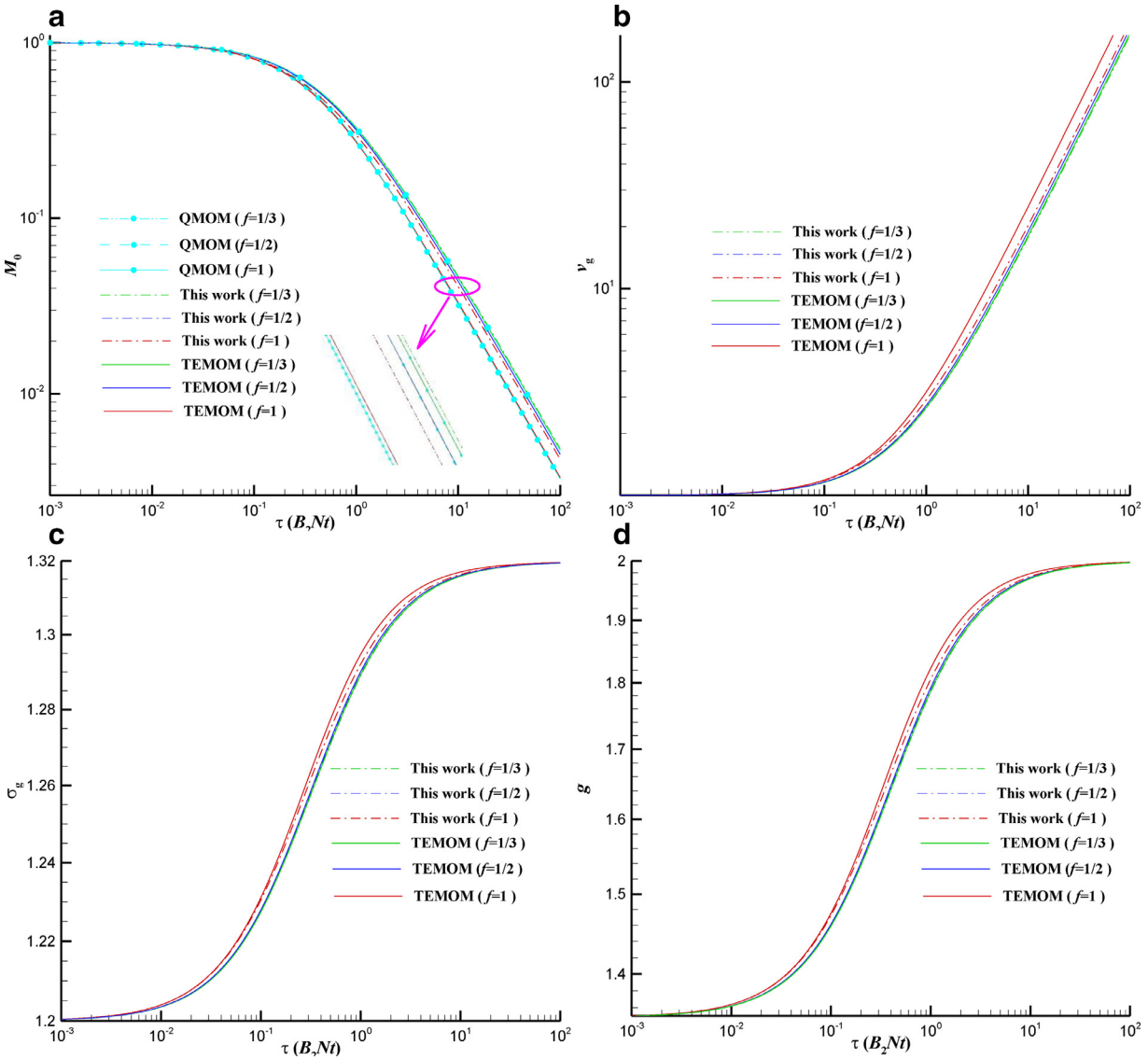

Fig. 2. Comparison of M_0 (a), v_g (b) σ_g (c), and g (d) obtained from this work with the TEMOM and QMOM models for $f=1$, 1/2, and 1/3.

4. Results and discussion

In this section, we verify the new analytical model by comparing it with other well-known numerical models for the same problem, including the TEMOM [26] and QMOM [8]. Here, the Gauss integral node number is 4 when the QMOM is implemented, and the Taylor-series expansion order is 3 when the TEMOM is implemented. Fig. 2 demonstrates the evolution of M_0, v_g, σ_g, and g with times obtained from these three methods for $f=1$,1/2, and 1/3, respectively. Notably, $f=1$,1/2, and 1/3 corresponds to the mass fractal dimension, $D_f=1$, 2, and 3. In this paper, v_g and σ_g are calculated as follows [33]:

$$v_g = {M_1}^2 \Big/ \left(M_0^{\frac{3}{2}} M_2^{\frac{1}{2}}\right), \tag{14}$$

and

$$\ln^2(\sigma_g) = \left(\frac{1}{9}\right) \ln(g). \tag{15}$$

For comparison, the same initial Kn (0.0001) and initial GSD (1.2) are selected for all cases. For M_0 as illustrated in Fig. 2(a), the results from the TEMOM and QMOM overlap for all three values of f; thus, the difference between them is negligible. Our study reveals that the difference of v_g, σ_g, and g between the TEMOM and QMOM is also negligible,

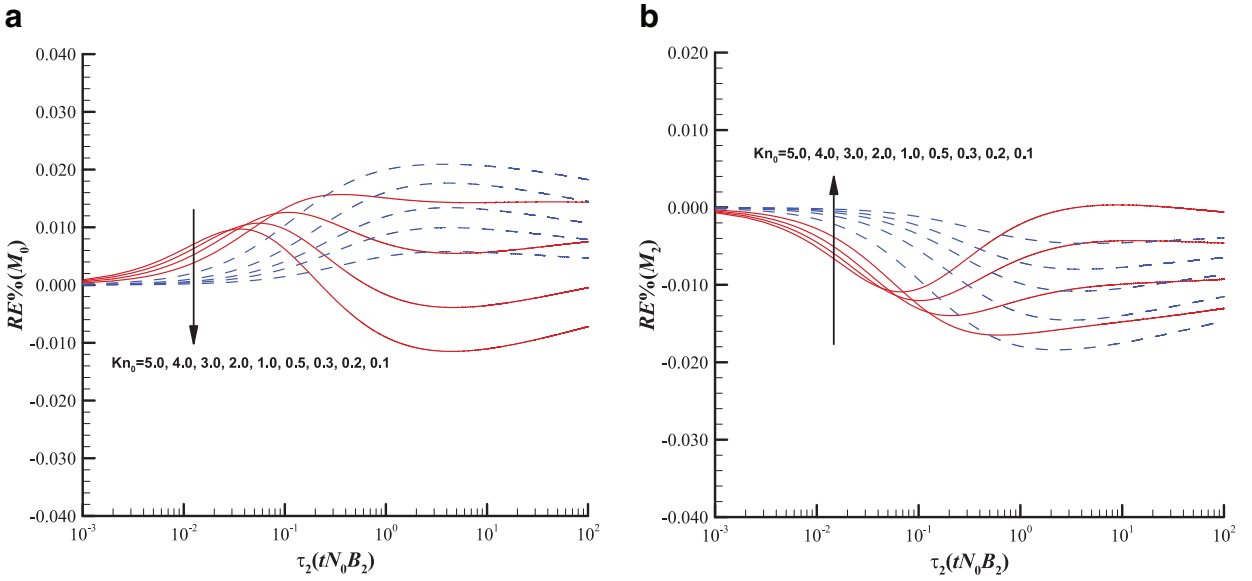

Fig. 3. Variance of the RE%s of the analytical solution with respect to the numerical solution for M_0 (a) and M_2 (b) that are relevant to dimensionless time in the near-continuum regime.

which is similar to Fig. 2(a) for M_0.Therefore, the results from the QMOM are not displayed in Fig. 2(b–d). The comparison between the TEMOM and QMOM verifies that selecting the TEMOM as the reference in this study is feasible. Comparing the analytical solution to the TEMOM illustrates a decreasing difference for all four investigated quantities, including M_0, v_g, σ_g, and g, with an increase of D_f (or decrease of f). This indicates that the accuracy of the analytical solution is affected by the mass fractal dimension. However, the difference between the proposed analytical solution and the TEMOM is not obvious. In fact, when $f=1/2$ and $1/3$, the difference between the two methods is negligible. Thus, the analytical method proposed in this work is verified as a reliable method for solving the agglomerate Brownian coagulation equation in the continuum-slip regime. Next, we further study the difference between the analytical solution and the TEMOM by selecting $f=1/3$ as an example and investigate how to improve the accuracy of the analytical solution.

4.1. Pseudo-self-preserving aerosols

The evolution of the aerosol size distribution in the continuum-slip regime exhibits notably different characteristics from those in the free molecular regime and continuum regime [21]. This difference occurs because the GSDs in the free molecular regime and continuum regime are unchanged values [9,11,22,36], whereas in the continuum-slip regime, particularly in the near-continuum regime from $Kn=0.1000$ to $Kn=5.0000$, the GSD always varies, even though the variance is limited to a notably small range, as reported in [21]. In the literature, the study on the constant GSD in both the continuum regime and free molecular regime is called the self-preserving theory, which was first proposed in [22]. In the continuum-slip regime, however, the GSD is not always constant, and, therefore, the size distribution of an aerosol in this regime was called a pseudo-self-preserving size distribution [36]. In this case, the asymptotic solution, which assumes GSD to be constant, becomes invalid [37].

To verify the newly proposed analytical solution in the near-continuum regime, the RE%s of the analytical solution to the TEMOM for M_0 and M_2 are presented in Fig. 3(a) and (b), where there are nine representative cases with Kn from 5.0000 to 0.1000 (5.0000, 4.0000, 3.0000, 2.0000, 1.0000, 0.5000, 0.3000, 0.2000, and 0.1000). In addition, to gather additional evidence for the conclusion from Fig. 3, the RE%s with much denser Kn (5.0000, 4.5000, 4.0000, 3.5000, 3.0000, 2.5000, 2.0000, 1.5000, 0.8000, 0.7000, 0.6000, 0.5000, 0.4000, 0.3000, 0.2000, 0.1000, and 0.0100)are displayed in Supplementary Fig. 1(a) and (b), where the data in Supplementary Data1 are used. The characteristics of the initial size distribution for the investigated cases are determined using three key quantities: Kn, GSD, and GMD, which are displayed in Table 1. These cases are selected to continuously span the entire near-continuum regime. In these cases, the GSDs are the values of pseudo-self-preserving aerosols [28].

In Fig. 3(a) and (b), the abscissa is operated with a log scale to clearly distinguish the curves. For both M_0 and M_2, their RE%s vary in a notably limited range, and their absolute values are always below 0.0200. The same conclusion is further verified in Supplementary Fig. 1(a) and (b), which contain much denser Kn numbers. For both M_0 and M_2, the RE%s approach their asymptotic values at approximately $\tau = 1.0000$ and subsequently remain at these values in the late stage, which indicates that the RE%s of the analytical solution to the referenced TEMOM are not amplified with time. This new characteristic of the proposed analytical solution ensures that the PBE dominated by Brownian coagulation can be very

Table 1
Characteristics of the investigated cases when the calculation is performed up to $\tau = 100$. (GSD denotes the geometric standard deviation; GMD denotes the geometric mean diameter (unit: nanometer); *Kn* denotes the Knudsen number.

No.	GMD	GSD	*Kn*
1	27.3653	1.3236	5.0000
2	34.2067	1.3169	4.0000
3	45.6089	1.3079	3.0000
4	68.4133	1.2986	2.0000
5	136.8266	1.2888	1.0000
6	273.6532	1.2904	0.5000
7	456.0887	1.2950	0.3000
8	684.1330	1.3000	0.2000
9	1368.2660	1.3065	0.1000

accurately solved using the proposed analytical solution, especially within a dimensionless time of 100.0000. In fact, for the physical parameters in Section 3, a dimensionless time of 100.0000 corresponds to a real time of 6.7056×10^4 s, when the initial total particle number concentration is 1.0000×10^{13} #/m^3, which is the typical concentration in nanoparticle synthesis engineering [38,39].

In the continuum regime, the variance of the RE%s of the proposed analytical solution to the referenced TEMOM for M_0 and M_2 are represented in Fig. 4(a) and (b), respectively. In this figure, the representative initial *Kn* (i.e., 0.100, 0.080, 0.060, 0.040, 0.020, 0.010, 0.005, and 0.001) are selected to cover the entire continuum regime. Similar to those in the previously investigated near-continuum regime, the RE%s for both M_0 and M_2 in Fig. 4 quickly approach their asymptotic values and remain at these values in the late stage. Although the absolute values of the RE%s for both M_0 and M_2 are always notably small (0.006 for M_0 and 0.005 for M_2), the variance of the RE%s with the initial *Kn* exhibits regularity. When the initial *Kn* decreases, the absolute value of the RE%s also decreases. Therefore, in the continuum regime, the precision of the proposed analytical solution increases with a decrease of the initial *Kn*. This result causes the GSD in the continuum regime to slowly approach a constant value of 1.3200 when the *Kn* decreases from 0.1000 which is consistent with the GSD findings in [21]. We compared Figs. 3 and 4 and discovered that the proposed analytical solution is more precise in the continuum regime than in the near-continuum regime. The main reason is that the GSD always varies with the *Kn* in the near-continuum regime, whereas in the continuum regime, it is nearly constant [34]. Notably, the division between the continuum regime and the near-continuum regime is slightly different from that reported in [34] regarding the *Kn* number. In this paper, the *Kn*, 0.1000, is defined as the division point for these two regimes following the work displayed in [24], whereas in [34], the *Kn* is lower than 0.1000.

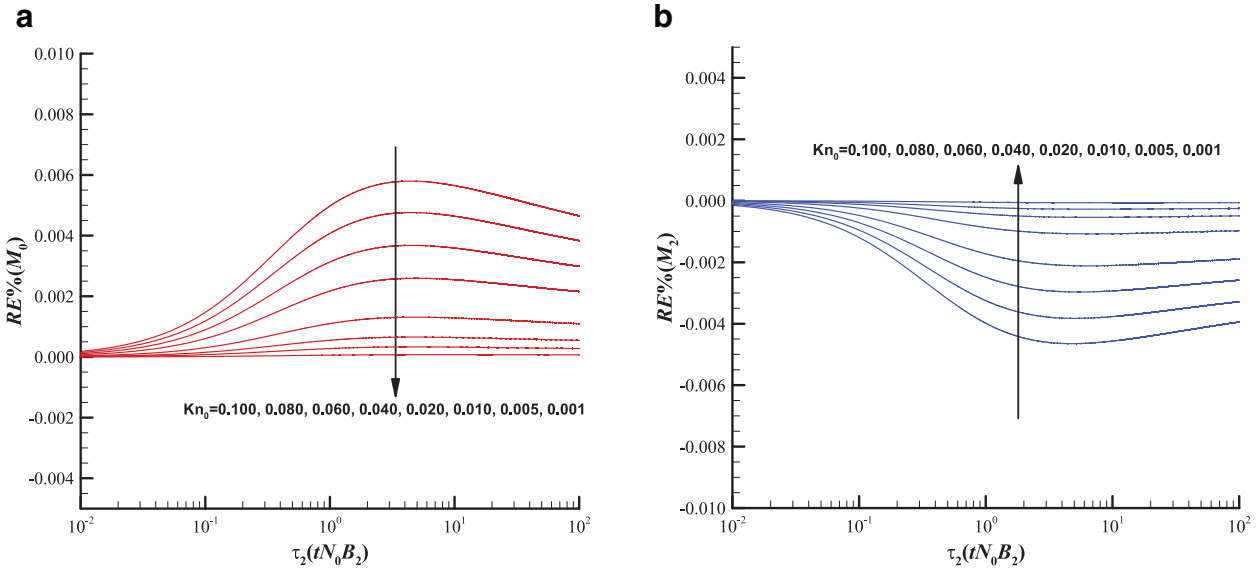

Fig. 4. Variance of the RE%s of the analytical solution to the referenced numerical solution for M_0 (a) and M_2 (b) that are relevant to the dimensionless time in the continuum regime.

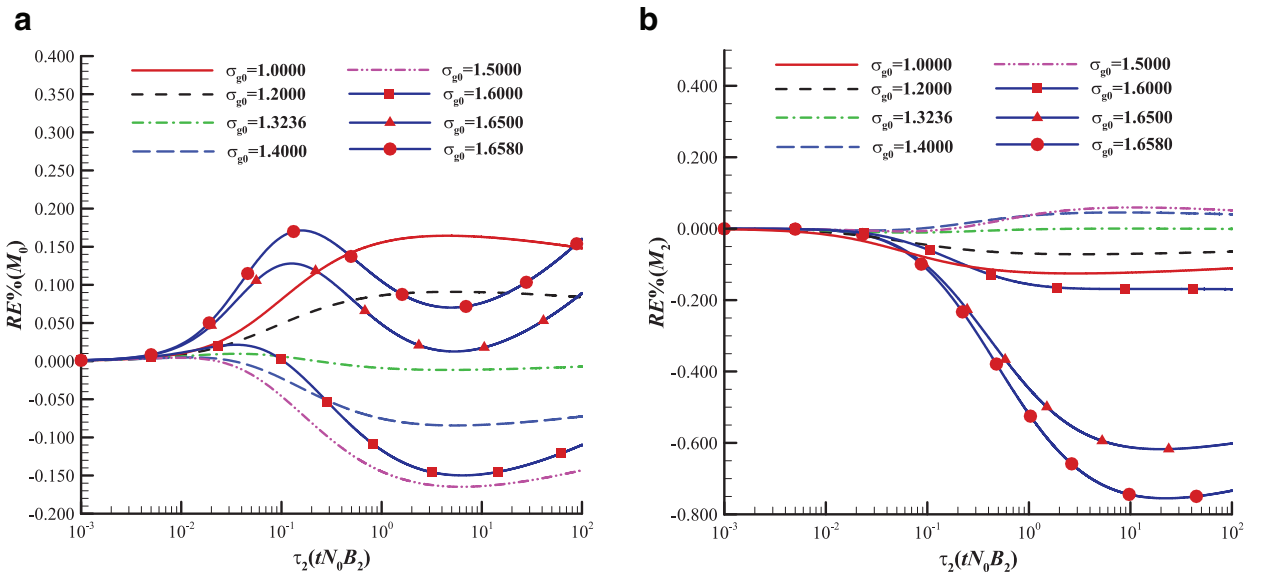

Fig. 5. Relative errors of the analytical method to the referenced numerical method for M_0 (a) and M_2 (b) with different initial GSDs when the initial Kn is 5.0000.

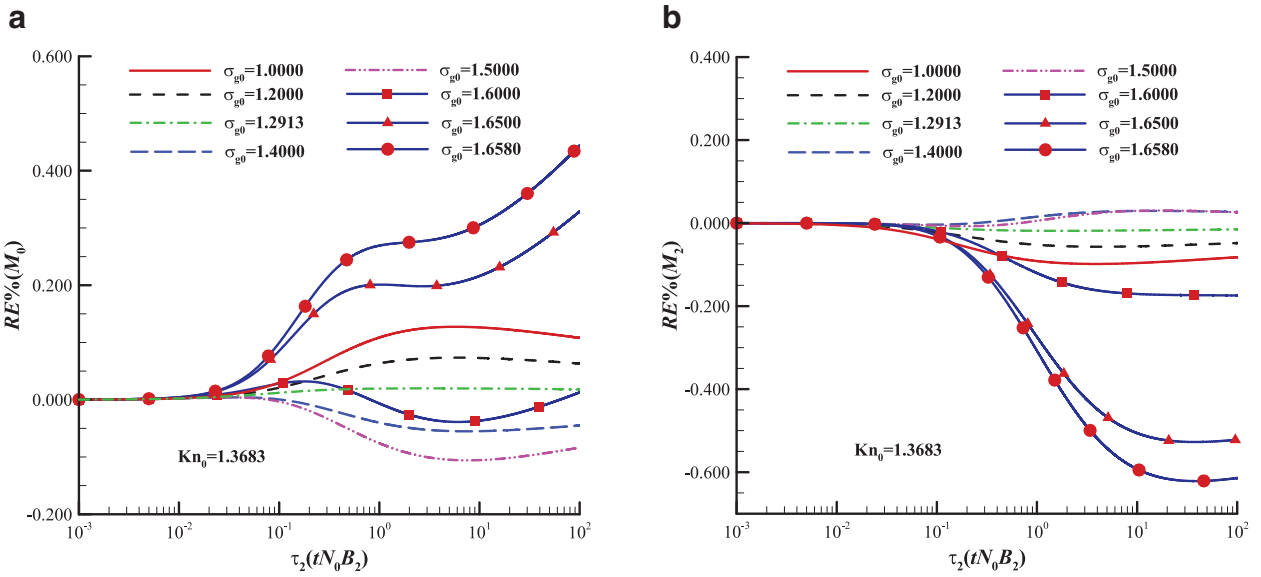

Fig. 6. Relative errors of the analytical method to the numerical method for M_0 (a) and M_2 (b) with different initial GSDs when the initial Kn is 1.3683.

4.2. Non-self-preserving aerosols

To study the deviation of the analytical solution from the TEMOM for non-self-preserving aerosols, two Kn of 5.0000 and 1.3683 are selected as the representative cases of the near-continuum regime, and three Kn of 0.0100, 0.0010, and 0.0001 are selected as the representative cases of the continuum regime.

The RE%s of the analytical solution to the referenced TEMOM for both M_0 and $M_2$when the initial Kn is 5.0000 are displayed in Fig. 5(a) and (b), respectively, where eight initial GSDs are investigated. The initial GSDs in the figure continuously span the entire validated GSD range from 1.0000 to 1.6583. Similarly, the RE%s of the analytical solution to the referenced TEMOM for both M_0 and M_2 are presented in Fig. 6(a) and (b), respectively, when the initial Kn is 1.3683. Notably, because the investigated aerosol is self-preserving, the GSD is 1.3236 in Fig. 3 and 1.2913 in Fig. 4. Both Figs. 5 and 6 illustrate that higher absolute values of the RE%s for M_0 and $M_2$are generated when the GSD deviates from the value of the

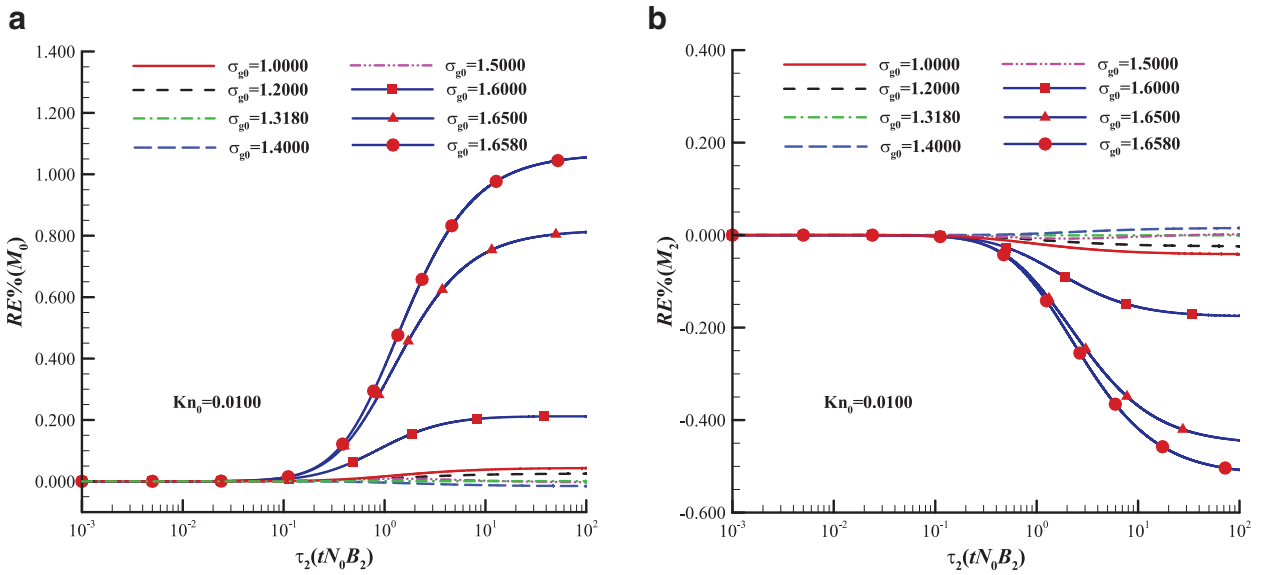

Fig. 7. Relative errors of the analytical method to the numerical method for M_0 (a) and M_2 (b) with different initial GSDs when the initial Kn number is 0.0100.

self-preserving aerosols, and there are asymptotic values when the GSD is below 1.5000. When the initial GSD is equal to or greater than 1.6000, the absolute values of the RE%s for M_0 do not converge to an asymptotic value with time; therefore, it is not necessary to determine the scope of the errors that are generated by the analytical solution. The analytical solution is not recommended for use in the near-continuum regime for non-self-preserving aerosols, particularly when the GSD is equal to or greater than 1.6000.

The RE%s of the analytical solution to the referencedTEMOM for both M_0 and $M_2$for the initial *Kn* 0.0100 are illustrated in Fig. 7(a) and (b), respectively. The RE%s for the initial *Kn* 0.0010 and 0.0001 are not displayed in this figure because the curves for the three *Kn* of 0.0100, 0.0010, and 0.0001 always overlap for each initial GSD, which cannot be distinguished from one another. Hence, the effect of the *Kn* on the RE% value is negligible in the continuum regimewhen the *Kn* is below 0.0100. In Fig. 7(a) and (b), the asymptotic values of theRE%s for both M_0 and M_2clearly exist for all initial GSDs; in particular, higher absolute values of the RE% are generated when the aerosol deviates more from its self-preserving status. Notably, the GSD at the self-preserving status is approximately 1.3200 in the continuum regime [11,21]. Because the RE%s only depend on the initial GSD, the relationship between the RE%s and the initial GSD must be determined to modify the analytical solution by introducing the RE%s to the original Eq. (11).

To identify the relationship between the initial GSD and the RE%, up to 36 GSDs are investigated for the *Kn* 0.0010.The RE%s of the analytical solution to the referenced TEMOM that are relevant to the initial GSDs are illustrated in Fig. 8(a) and (b) for M_0 and M_2, respectively. The data for the initial GSDs and the corresponding *RE%*s are attached online under the name "Supplementary-Data2."The relationship between the initial GSD and the *RE%* is represented by a mathematical equation by performing a 7th-degree polynomial fitting technique. In mathematics, the fitting function fits the initial data much more accurately if the selected polynomial degree has a higher value. Here, the mathematical equations that relate the initial GSD for both M_0 and M_2 to the RE% are,

$$f\left(\sigma_{g0}\right)_{m0} = 0.00530\omega^7 + 0.02600\omega^6 + 0.03900\omega^5 + 0.02300\omega^4 + 0.02700\omega^3 + 0.03900\omega^2 - 0.02300\omega - 0.01400, \tag{16}$$

$$f\left(\sigma_{g0}\right)_{m2} = -0.0023082\epsilon^7 + 0.019183\epsilon^6 - 0.066531\epsilon^5 - 0.13502\epsilon^4 - 0.19577\epsilon^3 - 0.19769\epsilon^2 - 0.071352\epsilon + 0.0093324, \tag{17}$$

with $\omega = (\sigma_{g0} - 1.40000)/0.19000$ and $\epsilon = (\sigma_{g0} - 1.4829)/0.19323$.$f(\sigma_{g0})_{m0}$ and $f(\sigma_{g0})_{m2}$ are functions of σ_{g0} that represent the relationship between the initial GSD and the RE% over the effective range of TEMOM ODEs. Correspondingly, the residuals in the curve-fitting performance are also illustrated in Fig. 8, the absolute values of which are always less than 2×10^{-3} for M_0 and 4×10^{-4} for M_2, which indicates that fitting Eqs. (9) and (10) are highly reliable. After Eqs. (16) and (17) are introduced into Eq. (11), the errors of the proposed analytical solution for non-self-preserving aerosols are largely reduced, and their precision can be ensured. The treatment is actually an asymptotic solution because it is only valid after the aerosol evolves over a long period of time, which is the same as in [37].

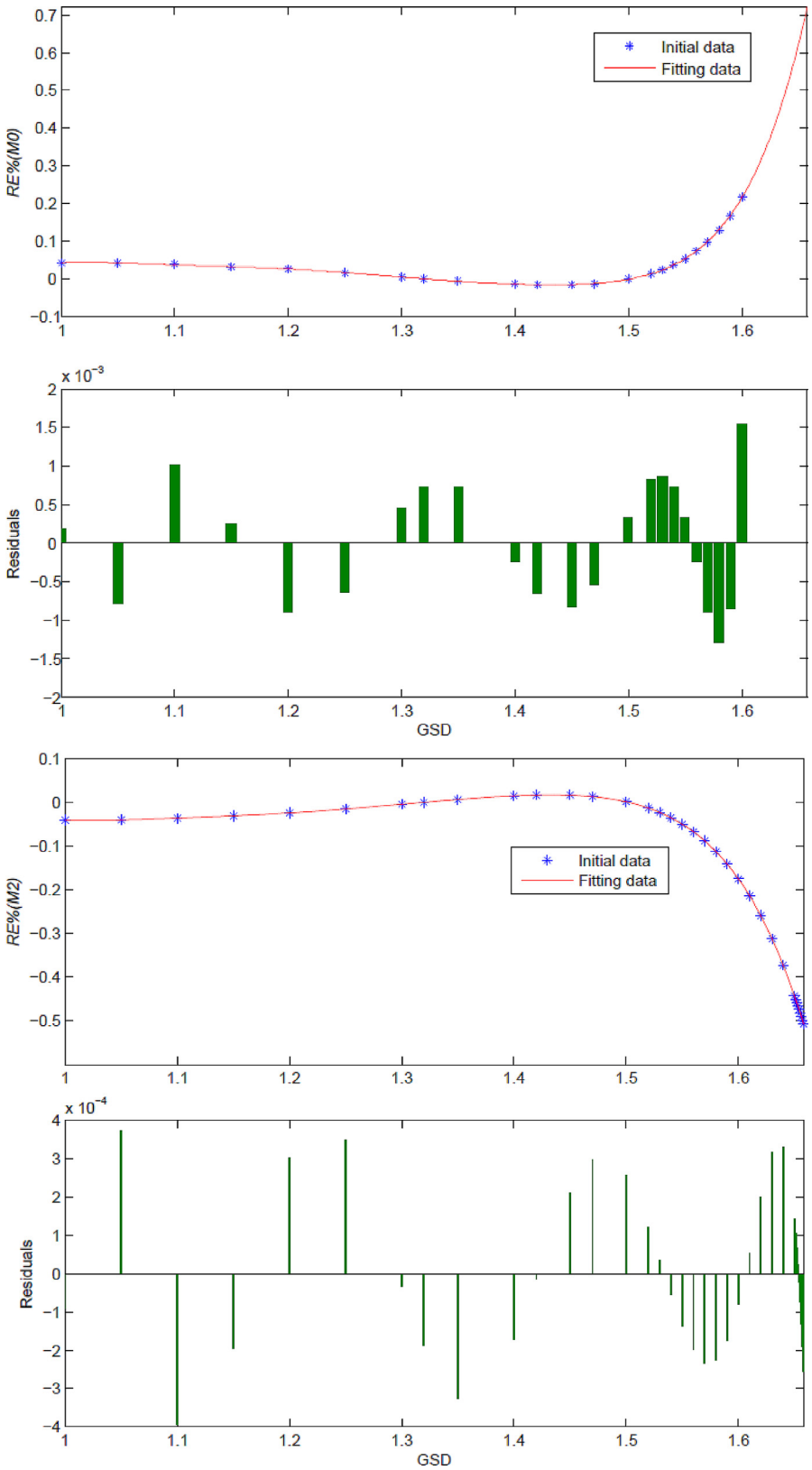

Fig. 8. Variance of the RE% of the analytical solution to the referenced numerical solution with the initial GSD and the residuals generated in the performance of the 7th-degree polynomial fitting operation for M_0 (a) and M_2 (b).

5. Conclusions

A new analytical solution for solving the PBE was first proposed, which is applicable to fractal-like agglomerates undergoing Brownian coagulation in the continuum-slip regime. The reliability of the new solution was verified by comparison with two highly accurate numerical solutions, namely the TEMOM and QMOM, with the mass fractal dimension specified as 1, 2, and 3. The solution indicates that, as the mass fractal dimension number increases, the difference between the analytical solution and the TEMOM decreases. The *Kn* number was discovered to play a crucial role in determining the accuracy of the new solution in this regime. For pseudo-self-preserving aerosols, the new analytical solution was verified as a very highly precise solution with very minor relative errors for both the zeroth and second moments. The proposed analytical solution was also verified as being able to solve the PBE for non-self-preserving aerosols with *Kn* below 0.0100 with highly reliable precision. For non-self-preserving aerosols with *Kn* greater than 0.0100, the new solution can be further improved by incorporating a GSD-dependent correction factor into the original mathematical formula. The newly developed solution was finally verified to have the potential to replace the numerical solution in the continuum-slip regime.

Acknowledgments

Dr. Yu thanks Zhejiang Provincial Natural Science Foundation of China under Grant no. LQ15A020002 and LQ16A020002, the Sino-German Research Project under Grant no. GZ971, and the Opening fund of the State Key Laboratory of Nonlinear Mechanics for financial support. The authors also express their gratitude for the joint support of the National Natural Science Foundation of China with nos. 11372299 and 51390490.

Supplementary materials

Supplementary material associated with this article can be found, in the online version, at doi:10.1016/j.apm.2016.01.009.

References

[1] C. Thornton, How do agglomerates break? Powder Technol. 144 (2004) 110–116.
[2] S.K. Friedlander, Smoke, Dust and Haze: Fundamentals of Aerosol Behavior, 2nd ed., John Wiley & Sons, Inc., 2000.
[3] D. Ramkrishna, M.R. Singh, Population balance modeling: current status and future prospects, Annu. Rev. Chem. Biomol. Eng. 5 (2014) 123–146.
[4] M. von Smoluchowski, Versuch einer mathematischen theorie der koagulationskinetik kolloider L{ö}sungen, Z. Phys. Chem 92 (1917) 9.
[5] H. Müller, Zur allgemeinen theorie ser raschen koagulation, Fortschr. Kolloide Polym. 27 (1928) 223–250.
[6] H.M. Hulburt, S. Katz, Some problems in particle technology: a statistical mechanical formulation, Chem. Eng. Sci. 19 (1964) 555–574.
[7] M. Frenklach, Method of moments with interpolative closure, Chem. Eng. Sci. 57 (2002) 2229–2239.
[8] R. McGraw, Description of aerosol dynamics by the quadrature method of moments, Aerosol Sci. Technol. 27 (1997) 255–265, doi:10.1080/02786829708965471.
[9] K.W. Lee, H. Chen, J.A. Gieseke, Log-normally preserving size distribution for Brownian coagulation in the free-molecule regime, Aerosol Sci. Technol. 3 (1984) 53–62.
[10] D.L. Marchisio, R.D. Vigil, R.O. Fox, Quadrature method of moments for aggregation-breakage processes, J. Colloid Interface Sci. 258 (2003) 322–334.
[11] M. Yu, J. Lin, T. Chan, A new moment method for solving the coagulation equation for particles in Brownian motion, Aerosol Sci. Technol. 42 (2008) 705–713.
[12] F. Gelbard, J. Seinfeld, Simulation of multicomponent aerosol dynamics, J. Colloid Interface Sci. 78 (1980) 485–501.
[13] S.S. Talukdar, M.T. Swihart, Aerosol dynamics modeling of silicon nanoparticle formation during silane pyrolysis: a comparison of three solution methods, J. Aerosol Sci. 35 (2004) 889–908.
[14] M. Kostoglou, Extended cell average technique for the solution of coagulation equation, J. Colloid Interface Sci. 306 (2007) 72–81.
[15] J.D. Landgrebe, S.E. Pratsinis, A discrete-sectional model for particulate production by gas-phase chemical reaction and aerosol coagulation in the free-molecular regime, J. Colloid Interface Sci. 139 (1990) 63–86.
[16] M. Kraft, Modelling of particulate processes, KONA 23 (2005) 18–35.
[17] N. Morgan, C. Wells, M. Goodson, M. Kraft, W. Wagner, A new numerical approach for the simulation of the growth of inorganic nanoparticles, J. Comput. Phys. 211 (2006) 638–658.
[18] H. Zhao, C. Zheng, A population balance-Monte Carlo method for particle coagulation in spatially inhomogeneous systems, Comput. Fluids 71 (2013) 196–207.
[19] H. Zhao, F.E. Kruis, C. Zheng, A differentially weighted Monte Carlo method for two-component coagulation, J. Comput. Phys. 229 (2010) 6931–6945.
[20] M. Xie, Q. He, Asymptotic solution of population balance equation based on TEMOM model, Chem. Eng. Sci. 94 (2013) 79–83.
[21] K. Lee, Y. Lee, D. Han, The log-normal size distribution theory for Brownian coagulation in the low Knudsen number regime, J. Colloid Interface Sci. 492 (1997) 486–492.
[22] S.K. Friedlander, C.S. Wang, The self-preserving particle size distribution for coagulation by Brownian motion, J. Colloid Interface Sci. 22 (1966) 126–132.
[23] U. Vogel, K. Savolainen, Q. Wu, M. van Tongeren, D. Brouwer, M. Berges, Handbook of Nanosafety: Measurement, Exposure and Toxicology, Elsevier, 2014.
[24] S. Pratsinis, Simultaneous nucleation, condensation, and coagulation in aerosol reactors, J. Colloid Interface Sci. 124 (1988) 416–427.
[25] J.C. Barrett, J.S. Jheeta, Improving the accuracy of the moments method for solving the aerosol general dynamic equation, J. Aerosol Sci. 27 (1996) 1135–1142.
[26] M. Yu, J. Lin, Taylor-expansion moment method for agglomerate coagulation due to Brownian motion in the entire size regime, J. Aerosol Sci. 40 (2009) 549–562.
[27] K.W. Lee, H. Chen, Coagulation rate of polydisperse particles, Aerosol Sci. Technol. 3 (1984) 327–334.
[28] M. Yu, J. Lin, H. Jin, Y. Jiang, The verification of the Taylor-expansion moment method for the nanoparticle coagulation in the entire size regime due to Brownian motion, J. Nanopart. Res. 13 (2011) 2007–2020.
[29] M. Xie, Q. He, The fundamental aspects of TEMOM model for particle coagulation due to Brownian motion. Part I: in the free molecule regimes, Int. J. Heat Mass Transf. 70 (2014) 1115–1120.
[30] M. Yu, Y. Liu, J. Lin, M. Seipenbusch, Generalized TEMOM scheme for solving the population balance equation, Aerosol Sci. Technol. 49 (2015) 1021–1036.

[31] M. Yu, M. Seipenbusch, J. Yang, H. Jin, A new analytical solution for solving the smoluchowski equation due to nanoparticle Brownian coagulation for non-self-preserving system, Aerosol Air Qual. Res. 14 (2014) 1726–1737.
[32] M. Yu, J. Lin, Solution of the agglomerate Brownian coagulation using Taylor-expansion moment method, J. Colloid Interface Sci. 336 (2009) 142–149.
[33] S.E. Pratsinis, Simultaneous nucleation, condensation, and coagulation in aerosol reactors, J. Colloid Interface Sci. 124 (1988) 416–427.
[34] S. Park, K. Lee, E. Otto, H. Fissan, log-normal size distribution theory of Brownian aerosol coagulation for the entire particle size range: Part I—analytical solution using the harmonic mean coagulation, J. Aerosol Sci. 30 (1999) 3–16.
[35] E. Otto, H. Fissan, S. Park, log-normal size distribution theory of brownian aerosol coagulation for the entire particle size range:: part II–analytical solution using Dahneke's coagulation kernel, J. Aerosol Sci. 30 (1999) 17–34.
[36] E. Otto, U. Drosten, H. Fissan, S.H. Park, K.W. Lee, Analytic solution of the coagulation equation for log-normal distributed aerosols in the entire size regime, J. Aerosol Sci. 29 (1998) S1283–S1284.
[37] Z. Chen, J. Lin, M. Yu, Asymptotic behavior of the Taylor-expansion method of moments for solving a coagulation equation for Brownian particles, Particuology 14 (2014) 124–129.
[38] B. Buesser, S.E. Pratsinis, Design of nanomaterial synthesis by aerosol processes, Annu. Rev. Chem. Biomol. Eng. 3 (2012) 103–127.
[39] M. Yu, J. Lin, H. Xiong, Quadrature method of moments for nanoparticle coagualtion and diffusion in the planar impinging jet flow, Chin. J. Chem. Eng. 15 (2007) 828–836.